Anatomy of inertial magnons in ferromagnetic nanostructures

Alexey M. Lomonosov [1,*] Vasily V. Temnov,[2,3,†] and Jean-Eric Wegrowe[3,‡]

[1]*Scientific and Technological Center of Unique Instrumentation, Russian Academy of Sciences, 117342, Butlerova street 15, Moscow, Russian Federation*

[2]*Institut des Molécules et Matériaux du Mans, UMR CNRS 6283, Le Mans Université, 72085 Le Mans, France*

[3]*LSI, Ecole Polytechnique, CEA/DRF/IRAMIS, CNRS, Institut Polytechnique de Paris, F-91128 Palaiseau, France*

(Received 11 May 2021; revised 1 August 2021; accepted 2 August 2021; published 18 August 2021)

We analyze dispersion relations of magnons in ferromagnetic nanostructures with uniaxial anisotropy taking into account inertial terms, i.e., magnetic nutation. Inertial effects are parametrized by the damping-independent parameter β, which allows for an unambiguous discrimination of inertial effects from Gilbert damping parameter α. The analysis of magnon dispersion relation shows its two branches are modified by the inertial effect, albeit in different ways. The upper nutation branch starts at $\omega = 1/\beta$, the lower branch coincides with ferromagnetic resonance (FMR) in the long-wavelength limit and deviates from the zero-inertia parabolic dependence $\simeq \omega_{\mathrm{FMR}} + Dk^2$ of the exchange magnon. Taking a realistic experimental geometry of magnetic thin films, nanowires, and nanodiscs, magnon eigenfrequencies, eigenvectors, and Q-factors are found to depend on the shape anisotropy. The possibility of phase-matched magnetoelastic excitation of nutation magnons is discussed and the condition was found to depend on β, exchange stiffness D, and the acoustic velocity.

DOI: 10.1103/PhysRevB.104.054425

I. INTRODUCTION

After the first description of the dynamics of the magnetization by Landau and Lifshitz [1], Gilbert proposed an equation that contained a correction due to the precessional damping [2,3]. Since then, the so-called Landau-Lifshitz-Gilbert (LLG) equation is known to give an excellent description of the dynamics of the magnetization, including ferromagnetic resonance (FMR) and magnetostatic waves [4,5], as well as the magnetization reversal [6,7]. Ferromagnetic resonance and time-resolved magnetization measurements allow its spatially homogeneous precession ($k = 0$), but also nonuniform modes of the magnetization precession ($k \neq 0$, where k is the wave vector of spin waves) to be measured [8–10]. During the last decades, these techniques have been advanced in the context of ultrafast demagnetization dynamics [11,12] that paved the way for the description of new physics at the sub-picosecond regime. High-frequency resonant modes of exchange magnons have been measured with ultrafast time-resolved optical techniques [8,10,13]. Therefore, the validity of the LLG equations has been confirmed down to the picosecond timescale and below.

However, the limitations of LLG equations were established in the stochastic derivation performed by Brown in a famous paper published in 1963 [14]. This limit is due to the hypothesis that the typical timescales of magnetization dynamics are much longer than those of other degrees of freedom forming the dissipative environment. In analogy to the common description of the diffusion process of a Brownian particle, the inertial (momentum) degrees of freedom are supposed to relax much faster than their spatial coordinates. This means that the degrees of freedom related to the linear momentum (in the case of the usual diffusion equation), or to the angular momentum (in the case of the magnetization) are included into the heat bath. As a consequence, the inertial terms do not explicitly appear in the equations, but are considered to be part of the damping term [15].

The possibility of measuring the contribution to inertial degrees of freedom led to a generalization of the LLG equation with an additional term, incorporating the second time-derivative of magnetization

$$\dot{\mathbf{m}} = -\gamma \mathbf{m} \times \mathbf{H}_{\mathrm{eff}} + \alpha \mathbf{m} \times \dot{\mathbf{m}} + \beta \mathbf{m} \times \ddot{\mathbf{m}}, \qquad (1)$$

where $\mathbf{m} = \mathbf{M}/M_s$ is the unit magnetization vector, M_s is the modulus of the magnetization which remains constant, $\gamma = \gamma_0 \mu_0$ is the product of the gyromagnetic ratio γ_0, and the vacuum permeability μ_0, α stands for the Gilbert damping. Inertial effects are characterized by the parameter β, which is introduced in a phenomenological way, i.e., independent of α and γ [16]. This generalized LLG equation has been derived in the framework of different and independent theoretical contexts [15,17–32]; its solutions were studied in a series of publications [33–36]. The main consequence of inertia for the uniform magnetization (magnon with the wave vector $k = 0$) is the existence of nutational motion that is superimposed on the precession. This leads to an appearance of the second resonance peak at a higher frequency in FMR spectra. The direct measurement of nutation was reported recently [37,38].

The goal of the present report is to study the consequences of these inertial effects on the exchange magnons (i.e., $k \neq 0$ modes), in the perspective of experimental studies. This work

*lom@kapella.gpi.ru
†vasily.temnov@polytechnique.edu
‡jean-eric.wegrowe@polytechnique.edu

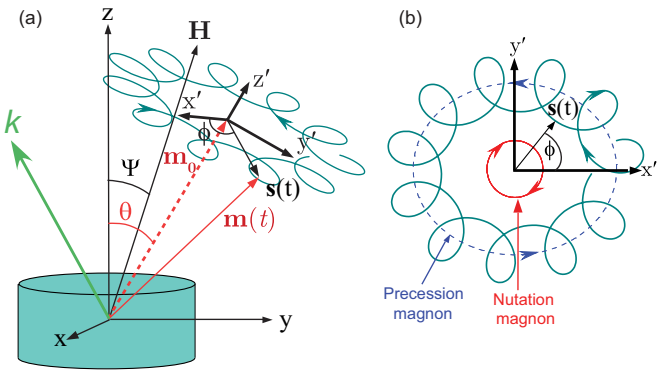

FIG. 1. (a) Inertial magnons propagating in ferromagnetic nanostructures under an external magnetic field **H** result in complex magnetization dynamics. (b) They can be decomposed in precession magnon and nutation magnon circulating in opposite directions on elliptical trajectories at different frequencies, giving rise to a characteristic *flower-shaped* trajectory.

is restricted to the infinitesimal linear excitations governed by exchange interaction in ferromagnets at the micromagnetic limit. This work completes the first description published in 2015, Sec. IV of the remarkable work of Kikuchi and Tatara [22], and independently reconsidered by Makhfudz *et al.* in 2020 [39].

The paper is organized as follows. Section II presents the derivation of the linear magnetic excitations deduced from Eq. (1). Section III describes the dispersion relation in a simple case of zero dipolar field (spherical symmetry). The first consequence of the inertia is that the dispersion relation splits in two branches: the lower one $s_1\exp(ikz - i\omega_1 t)$ (*precession magnons*) and the upper one for $s_2\exp(ikz - i\omega_2 t)$ (*nutation magnons*). The second consequence is that the quality factor Q increases with the k-vector. Section IV generalizes the description to the case of a uniaxial anisotropy quantified by the dimensionless (shape) anisotropy parameter ξ. In the anisotropic case the trajectories of both precession and nutation magnons become elliptical and rotating in opposite directions at each point in space. For a given k-vector the magnetization vector corresponding to a superposition of both magnons draws a typical trochoidal trajectory (see Fig. 1). Section V discusses the conditions for phase-matched excitation the nutation magnons by copropagating longitudinal acoustic phonons, illustrated by the material parameters for Gd-doped Permalloy thin films [13].

II. EXCHANGE MAGNONS IN FERROMAGNETIC THIN FILMS WITH MAGNETIC INERTIA

We start with the LLG equation for unit magnetization vector $\mathbf{m}$ with an effective field $\mathbf{H}_{\text{eff}}$, which includes an exchange interaction with stiffness D, an external field $\mathbf{H} = (H_x, 0, H_z)$ and a demagnetizing field induced by the shape anisotropy $\mathbf{H_d} = -M_S\widehat{N}\mathbf{m}$. The demagnetization tensor $\widehat{N}$ depends on the specific shape of the ferromagnetic sample. Hereafter we assume the diagonal form of $\widehat{N}$ with diagonal elements N_x, N_y, and N_z. Damping of the magnetization dynamics is described by the conventional Gilbert term with parameter α. In addition to the conventional LLG equation we take into account the inertial effect characterized by the independent parameter β. Then the inertial LLG equation (ILLG) takes the form of Eq. (1) with $\mathbf{H}_{\text{eff}} = \mathbf{H} + D\Delta\mathbf{m} + \mathbf{H_d}$.

The coordinate system was chosen such that the external field lies in the $y = 0$ plane, as is shown in Fig. 1. The material is assumed to be magnetically isotropic, so that the unperturbed magnetization vector also lies in the $y = 0$ plane. We seek for time- and space-dependent solutions in the form $\mathbf{m} = \mathbf{m_0} + \mathbf{s}(\mathbf{r}, \mathbf{t})$ with spin-wave solutions

$$\mathbf{s}(\mathbf{r}, t) = (s_x, s_y, s_z)\exp(i\mathbf{kr} - i\omega t), \tag{2}$$

propagating as a plane wave with a real wave vector $\mathbf{k}$, see Fig. 1. The substitution $\mathbf{m}(\mathbf{z}, \mathbf{t})$ into Eq. (1) and its linearization with respect to small perturbations s_x, s_y, s_z results in a homogeneous system of three linear equations

$$\widehat{A}\begin{pmatrix} s_x \\ s_y \\ s_z \end{pmatrix} = 0, \tag{3}$$

where the matrix A is given by

$$\begin{pmatrix} -i\omega & A_{12}(\omega, \mathbf{k}) & 0 \\ A_{21}(\omega, \mathbf{k}) & -i\omega & A_{23}(\omega, \mathbf{k}) \\ 0 & A_{32}(\omega, \mathbf{k}) & -i\omega \end{pmatrix}, \tag{4}$$

with coefficients $A_{ij}(\omega, \mathbf{k})$ defined as

$$\begin{aligned} A_{12} &= m_z(\gamma Dk^2 + \gamma M_S\xi_{yz} - i\alpha\omega - \beta\omega^2) + \gamma H_z, \\ A_{21} &= -m_z(\gamma Dk^2 + \gamma M_S\xi_{xz} - i\alpha\omega - \beta\omega^2) + \gamma H_z, \\ A_{23} &= m_x(\gamma Dk^2 + \gamma M_S\xi_{zx} - i\alpha\omega - \beta\omega^2) + \gamma H_x, \\ A_{32} &= -m_x(\gamma Dk^2 + \gamma M_S\xi_{yx} - i\alpha\omega - \beta\omega^2) - \gamma H_x, \end{aligned} \tag{5}$$

where coefficients $\xi_{ij} = N_i - N_j$ characterize the shape anisotropy. Note that the matrix elements depend on the wave-vector squared and not on its components, therefore all the properties related to its eigenvalues are independent of the propagation direction of the magnon. The condition for the nontrivial solution of the homogeneous system (3) to exist, i.e., $\det A = 0$, gives rise to the secular equation

$$\omega^2 + A_{12}(\omega, k)A_{21}(\omega, k) + A_{23}(\omega, k)A_{32}(\omega, k) = 0, \tag{6}$$

which is used to calculate the spin-wave dispersion relation $\omega(k)$ for different shapes/symmetries, i.e., characterized by different types of the $\widehat{N}$ tensor.

III. INERTIAL EXCHANGE MAGNONS IN SAMPLES WITH SPHERICAL SYMMETRY

Examples of such symmetry are infinite homogeneous isotropic ferromagnetic media, or any spherical body. In these cases the demagnetization tensor $\widehat{N}$ is diagonal with all nonzero elements equal 1/3, so that its contribution to the magnetization dynamics (1) and correspondingly to the wave matrix components (5) vanishes. The secular equation (6) takes a concise form

$$\begin{aligned} &\left(\gamma H + \gamma Dk^2 - \beta\omega^2 - i\alpha\omega + \omega\right) \\ &\times\left(\gamma H + \gamma Dk^2 - \beta\omega^2 - i\alpha\omega - \omega\right) = 0. \end{aligned} \tag{7}$$

Due to the symmetry of $\widehat{N}$, Eq. (7), and hence all its roots, remains independent on the direction of **H** and the equilibrium magnetization $\mathbf{m}_0$ with respect to the wave propagation direction along the z-axis. For each positive wave number k, the determinant (7) is solved for ω. Given that the presumed solution has a form $\sim\exp(ikz - i\omega t)$, positive ω designates the waves traveling in the positive direction. The two positive roots corresponding to the first parenthesis in Eq. (7) have the following forms:

$$\omega_1 = \frac{1}{2\beta}(-1 - i\alpha + \sqrt{4\gamma\beta(Dk^2 + H) + (1 + i\alpha)^2}), \quad (8)$$

$$\omega_2 = \frac{1}{2\beta}(1 - i\alpha + \sqrt{4\gamma\beta(Dk^2 + H) + (1 - i\alpha)^2}). \quad (9)$$

The first root is the lower magnon branch or precession, slightly modified by the inertial term, and the second one exhibits the inertial magnon branch or nutation. It is convenient to split these roots into real and imaginary parts: $\omega_{1,2} = \omega'_{1,2} + i\omega''_{1,2}$. The Taylor series approximation of those roots assuming the smallness of $\gamma\beta Dk^2, \gamma\beta H, \alpha \ll 1$ results in the following expressions for their real parts:

$$\omega'_1 \approx \gamma[Dk^2 + H - 2\beta\gamma HDk^2 + \cdots], \quad (10)$$

$$\omega'_2 \approx \frac{1}{\beta} + \omega'_1. \quad (11)$$

In this approximation the nutation magnon branch is simply shifted by $1/\beta$ with respect to precession magnon branch. The validity of this approximation is illustrated in Fig. 2(a), where frequencies $f = \omega/(2\pi)$ of the exact roots given by Eqs. (8) and (9) are depicted with solid lines, whereas dashed lines represent the power series approximation of Eqs. (10) and (11).

Lower branch emerges from the Larmor's frequency γH and grows parabolically with k. The effect of inertia reduces the coefficient at the term quadratic in k. The upper branch is simply displaced by $+1/\beta$ and has the similar shape. Imaginary parts of the roots $\omega''_{1,2}$ represent attenuation of the corresponding magnetization dynamics in time as $\propto \exp(\omega''_{1,2}t)$, and therefore they must be negative. In the frequency domain they characterize the width $\Delta f = |\omega''|/\pi$ [full width at half maximum (FWHM)] of the Lorentzian spectral line

$$\omega''_1 \approx -\alpha\gamma[Dk^2 + H - 6\beta\gamma HDk^2 + \cdots], \quad (12)$$

$$\omega''_2 \approx -\frac{\alpha}{\beta} - \omega''_1. \quad (13)$$

Note that in the limiting case of Eqs. (12) and (13) field and exchange stiffness have opposite effects on the attenuation of the two magnon branches: they increase the attenuation in the lower branch ω_1 and decrease it for the inertial branch ω_1. In the other limiting case of large-field and large-k attenuation of both branches tends to $\exp(-\frac{\alpha}{2\beta}t)$. The damping for both branches appears to be naturally proportional to the Gilbert damping parameter α. A conspicuous decrease of nutation linewidth $\omega''_2(k = 0)$ with growing α reported by Cherkasski *et al.* [36] roots back to the parametrization of the nutation phenomenon in terms of a product $\alpha\tau$, where τ denotes the characteristic nutation lifetime. Within this parametrization,

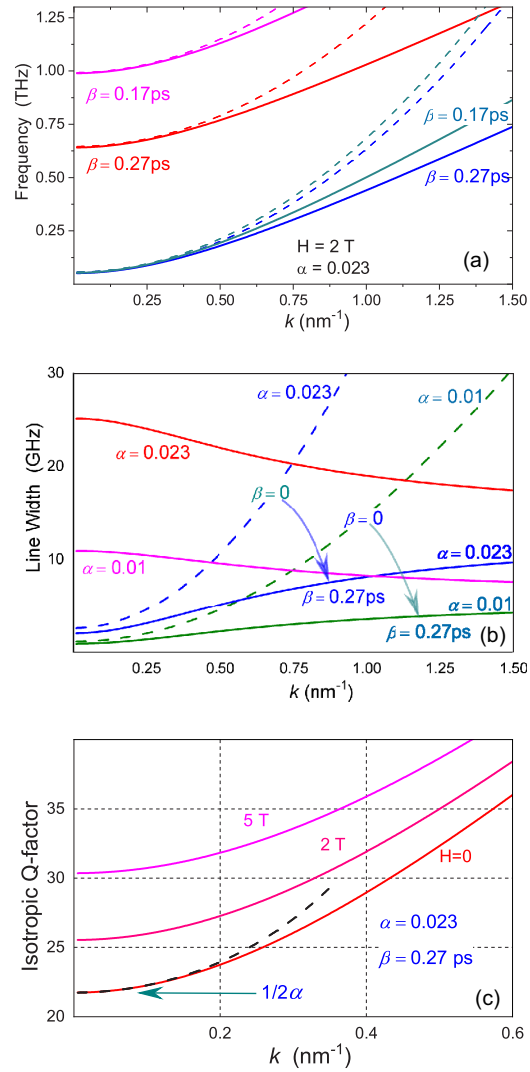

FIG. 2. (a) Dispersion of the nutation magnon (red, magenta) and precession magnon (blue, green). Dashed curves shows the approximations by Eqs. (10) and (11). (b) Corresponding line widths. To indicate the effect of inertia on the precession, dashed curves show the line width without inertia $\beta = 0$. (c) Quality factors $Q(k)$ for H in the range from zero to 5 T. The curve $2T$ corresponds to panels (a) and (b). Dashed curve is the approximation given by Eq. (14)

a variation of α, while keeping τ constant, leads to the simultaneous decrease of the nutation frequency $1/\beta = 1/(\alpha\tau)$ rendering the analysis of damping extremely difficult. An alternative notation in terms of α and β, introduced in this paper, resolves this problem and allows for an independent investigation of inertial and damping effects.

Another parameter, which characterizes the resonant spectral line centered at frequency f_0, is its quality factor defined as $Q = f_0/\Delta f = \omega'/(2\omega'')$. As can be seen from Eqs. (8) and (9), in isotropic ferromagnets Q-factors for both branches coincide within the accuracy of $\sim(\omega\alpha)^2$. The dependence of the Q-factor on the wave number k looks counterintuitive in that it essentially grows with k. Assuming for simplicity $H = 0$, for small k the Q-factor can be approximated by expansion of

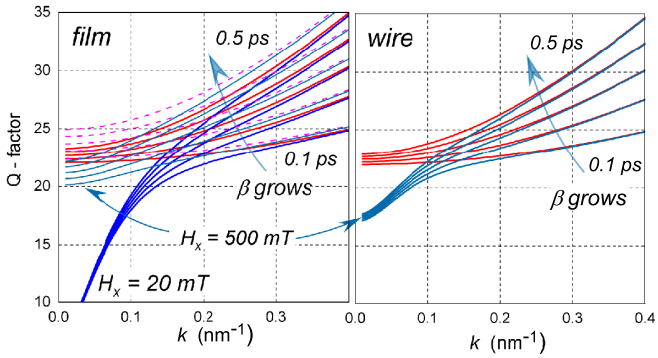

FIG. 3. Q-factor dependencies of precession branches (blueish lines) and nutation branches (reddish lines) and on k in a thin film and a wire for β ranging from 0.1 ps to 0.5 ps and in-plane magnetization $\mathbf{m}_0 = (1, 0, 0)$ and field $\mathbf{H} = (H_x, 0, 0)$. In a film (left panel) the Q-factor is plotted for two values $H_x = 20$ mT and 500 mT. In the wire (right panel) the field was 500 mT, which ensures saturation of magnetization

ω' and ω'' in the power series in k, which results in

$$Q(k) \sim \frac{1}{2\alpha}\frac{1+\gamma\beta Dk^2}{1-\gamma\beta Dk^2} + \cdots \sim \frac{1}{2\alpha}(1+2\gamma\beta Dk^2). \quad (14)$$

Exact values for the Q-factor in comparison to the estimate of Eq. (14) are shown in Fig. 3 for the external field ranging from 0 to 5 T.

The applied field helps to increase the quality factor; the effect for small k can be approximated as $Q \sim \sqrt{1+4\gamma\beta H + 4D\beta\gamma k^2}/(2\alpha)$.

IV. INERTIAL EXCHANGE MAGNONS IN SAMPLES WITH CYLINDRICAL SYMMETRY

Examples of such bodies are disks, wires, infinite plates, and films. Axial symmetry about the z-axis retains the diagonal form of $\widehat{N}$ with the diagonal elements satisfying the following conditions: $N_x = N_y$ and $N_x + N_y + N_z = 1$. As a result, the components of the matrix $\widehat{A}$ given by Eq. (5) acquire terms proportional to γM_S. The lack of symmetry makes the magnon propagation dependent on the orientation of vectors $\mathbf{m}_0$ and $\mathbf{H}$ with respect to the z-axis. We consider two limiting cases: collinear arrangement with $\mathbf{m}_0$ parallel to the axis of symmetry z ($\Theta = \Psi = 0$ in Fig. 1) and orthogonal arrangement with $\mathbf{m}_0$ parallel to the x-axis and $\Theta = \Psi = \pi/2$. In the collinear case the demagnetizing field acts simply against the external field, hence the secular equation remains similar to Eq. (7), but with field H substituted with the reduced field $H' = H - \xi M_S$:

$$(\gamma H' + \gamma Dk^2 - \beta\omega^2 - i\alpha\omega + \omega) \times (\gamma H' + \gamma Dk^2 - \beta\omega^2 - i\alpha\omega - \omega) = 0, \quad (15)$$

where $\xi = N_z - N_x = N_z - N_y$ characterizes the shape effect on demagnetizing, so that in an infinite wire $\xi = -1/2$ in the spherical symmetric (or unbounded) body $\xi = 0$ and in the infinite film $\xi = 1$. Correspondingly the roots to Eq. (15) are similar to the ones given in Eqs. (8) and (9) with modified field

$$\omega_1 = \frac{1}{2\beta}\left(-1 - i\alpha + \sqrt{4\gamma\beta(Dk^2 + H') + (1+i\alpha)^2}\right), \quad (16)$$

$$\omega_2 = \frac{1}{2\beta}\left(1 - i\alpha + \sqrt{4\gamma\beta(Dk^2 + H') + (1-i\alpha)^2}\right). \quad (17)$$

At the low-k limit the lower branch roughly tends to the Larmor's frequency $\gamma(H - \xi M_S)$ and the upper branch limit is $1/\beta + \gamma(H - \xi M_S)$, which is similar to the case of spherical symmetry, but with modified field. In the orthogonal configuration with $\mathbf{m}_0$ and $\mathbf{H}$ perpendicular to the axis of symmetry, the roots of the determinant (4) generally cannot be found in an analytical form. Therefore we first consider an approximate solution, and then describe briefly the numeric algorithm for obtaining the dispersion curves. By neglecting the Gilbert attenuation ($\alpha = 0$), the approximate solutions to Eq. (4) for the in-plane magnetization and field can be found in a concise analytical form:

$$\omega_{1,2} = \frac{1}{\beta\sqrt{2}}\{2\gamma\beta(Dk^2 + H) + \gamma\beta\xi M_s + 1, \mp\sqrt{4\gamma\beta(Dk^2 + H) + (\gamma\beta\xi M_s + 1)^2}\}^{1/2}. \quad (18)$$

Here indices 1 and 2 denote the frequencies of precession and nutation magnons, respectively. The minus sign prior to the square root in Eq. (18) corresponds to the precession branch ω_1; the plus sign denotes the nutation branch ω_2. Damping gives rise to the imaginary part of solutions (18), which for the small k limit and in-plane applied field $H_z = 0$, $H_x = H$ can be approximated as $\omega_1'' \approx -\alpha\gamma[\xi M_S(m_x^2/2 - m_z^2) + Hm_x]$ with the influence of β negligible in this approximation, as shown in Fig. 3. Components m_x, m_z minimize the free energy $M_S(m_x^2 N_x + m_z^2 N_z)/2 - Hm_x = \min$. In a film $m_x = 1, m_z = 0$, in a wire m_x grows with field as $m_x = 2H/M_S$ for $0 < H < M_S/2$ and $m_x = 1$ for $H \geqslant M_S/2$. The quality factor of the low-frequency branch is given by

$$Q_\perp|_{k=0} \approx \frac{\sqrt{H(\xi M_S m_x + H) + \xi^2 M_S^2 m_z^2}}{\alpha\left(\xi M_S m_x^2 + 2Hm_x - 2\xi M_S m_z^2\right)}. \quad (19)$$

In the case of spherical symmetry with $\xi = 0$ the quality factors of both branches are equal and tend to $1/(2\alpha)$ as shown in Fig. 2(c), whereas in a film ($\xi = 1$) or wire ($\xi = -1/2$) the quality factor of the precession magnon decreases at small k as shown in Fig. 3. In the in-plane magnetized film $m_z = 0$ the quality factor for the precession magnon with wave number k reduces to

$$Q_\perp|_f = \frac{\sqrt{D^2k^4 + Dk^2(M_S + 2H) + HM_S + H^2}}{\alpha(2Dk^2 + M_S + 2H)}. \quad (20)$$

Similarly to the case of spherical symmetry, in films and wires the inertial effect increases the quality factors of both branches as shown in Fig. 3.

The numerical procedure for building the dispersion relations of the magnonic modes for nonzero α or arbitrary orientation of the external field H starts with the calculation of the stationary equilibrium magnetization $\mathbf{m}_0 = (m_x, m_y, m_z)$.

This can be done by solving Eq. (1) in its stationary form, i.e., with all time derivatives set to zero. In a thin film, for example, quantities H_i and m_j are related by $M_S m_x m_z + H_x m_z - H_z m_x = 0$. Thus obtained stationary magnetization components are then substituted into Eqs. (5) and (4). At some fixed small k the determinant (4) as a function of complex-valued ω possesses two minima, which correspond to the precession and nutational branches. Their exact locations can be evaluated by a numerical routine which minimizes the absolute value of the determinant (4) in the vicinity of the guess values for those branches, for example, given by Eqs. (21) and (22). Then we give k a small increment and repeat the extremum search using the ωs obtained at the previous step as guess values and so on. As a result, the calculated values for ω_1 and ω_2 follow the dispersion curves of both branches. Note that for nonzero α roots $\omega_{1,2}$ possess imaginary parts, which determine the line width and Q-factor for each mode. Let us consider the magnetization behavior in a thin film in more detail. For this geometry $\widehat{N}$ possesses the only a nonzero component $N_z = 1$, and correspondingly, $\xi = 1$. In the small-k limit, the lower branch approaches the Kittel's frequency $\omega_{\mathrm{FMR}} = \gamma\sqrt{H(H+M_S)}$ from below as $\beta, k \to 0$:

$$\omega_1 \approx \omega_{\mathrm{FMR}} - \tfrac{1}{2}\gamma\omega_{\mathrm{FMR}}(2H + M_S)\beta + \cdots . \tag{21}$$

The effect of the demagnetizing field on the inertial branch is exhibited by an upward shift by $\frac{1}{2}\gamma M_S$; whereas the effect of inertia is the opposite:

$$\omega_2 \approx \frac{1}{\beta} + \gamma H + \frac{1}{2}\gamma M_S - \left(\omega_{FMR}^2 + \frac{1}{8}\gamma^2 M_S^2\right)\beta + \cdots . \tag{22}$$

For the orthogonal configuration, when both $\mathbf{m}_0$ and $\mathbf{H}$ lie in the film plane, we can estimate the trajectories of the magnetization dynamics of both modes for small k and small α. For each root given by Eq. (18) we solve the homogeneous equation for perturbations s (3). Normalization of the solutions can be chosen in an arbitrary way, here for simplicity we define $s_z = 1$. In orthogonal geometry the s_x component is obviously negligible or equals zero, so the system reduces to two equations in s_y and s_z. The results shown as a power series expansion for small inertia $\beta\omega \ll 1$ for the precession

$$s_p = \begin{pmatrix} 0 \\ -i\sqrt{1 + \frac{\xi M_S}{Dk^2+H}\left(1 + \frac{\beta\gamma\xi M_S}{2}\right)} \\ 1 \end{pmatrix} \exp(-i\omega_1 t), \tag{23}$$

and nutation

$$s_n = \begin{pmatrix} 0 \\ i(1 - \beta\gamma\xi M_S/2) \\ 1 \end{pmatrix} \exp(-i\omega_2 t), \tag{24}$$

with the parameter of anisotropy $\xi = 1$ for a thin film normal to the z-axis and $\xi = -1/2$ for a thin wire spread along the z-axis. Both perturbations exhibit elliptical polarization within the (x', y') plane. Precession trajectory is deformed by the demagnetizing effect so that the y-axis of the ellipse is stretched with the $\sqrt{1 + M_S/H}$ factor due to demagnetizing effect, and in addition by a factor of $1 + \xi\gamma\beta M_S/2$ on account of the inertial effect. On the contrary, the nutation ellipse is squeezed along the y-axis by the product of both parameters $\beta\xi$ as

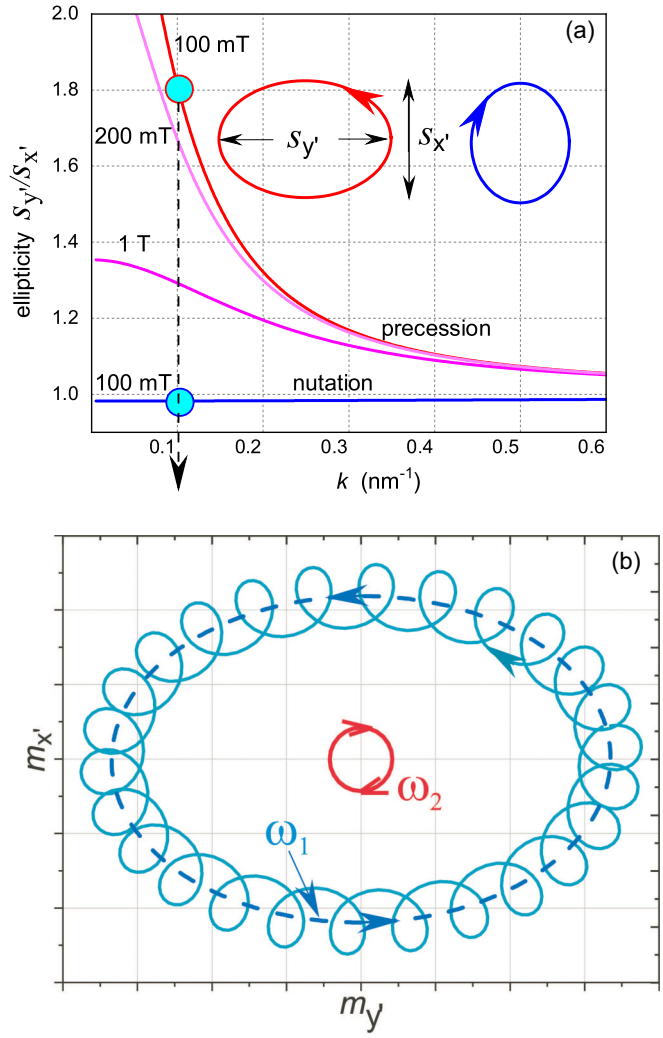

FIG. 4. Ratio of the polarization axes for the external field of 0.1 T, 0.2 T, and 1 T. **H** and $\mathbf{m}_0$ are parallel to the inward normal to the figure plane.

$1 - \xi\gamma\beta M_S/2$. The ellipticity of the lower branch depends on the external field (23), whereas that of the upper branch in this approximation shows no dependence on the field. The signs of the s_y components are opposite for nutation and precession; this indicates that they are rotating in the opposite directions. Exact polarizations can be found numerically for a reasonable set of material parameters and fields, as is shown in Fig. 4.

V. EXCITATION MECHANISMS OF INERTIAL EXCHANGE MAGNONS

The only experimental evidence of inertial effects in ferromagnets has been reported for $k = 0$ nutation mangons in Py-thin films resonantly excited with a magnetic field of an intense quasimonochromatic THz pulse [37]. To excite $k \neq 0$ exchange magnon modes one would need to have either spatially localized and instantaneous stimuli [10] or any other source of effective magnetic field characterized by spectral and spatial overlap with investigated magnon modes. The letter can be provided through ultrashort large-amplitude acoustic pulses [40,41] producing effective magnetoelastic

fields rapidly varying in time and space [42]. Acoustic pulses propagating through a thin ferromagnetic sample at an acoustic velocity v are quantified by a linearized dispersion relation $\omega_{ac} = vk$. Crossing between acoustic and magnon branches, i.e., satisfying the phonon-magnon phase-matching condition, usually facilitates the acoustic excitation of magnetization dynamics [43,44]. A question arises under which conditions the crossing between dispersion curves for longitudinal phonons and inertial magnons can occur. Whereas for realistic magnetic fields the acoustic dispersion always intersects the lower dispersion branch at a frequency close to FMR frequency [42]; the crossing of the upper nutation brunch is less obvious.

It is possible to quantify the criterion for magnetoelastic crossing with nutation magnons analytically. To do that we note that for larger wave numbers k satisfying $Dk^2 \gg H, M_S$ the exchange term plays the dominant role and the asymptotic behavior for both branches becomes linear in k:

$$\omega_{1,2} \approx \mp\frac{1}{2\beta} + k\sqrt{\frac{\gamma D}{\beta}}. \tag{25}$$

It follows from Eq. (25) that the condition for the nutation magnon branch to intersect the acoustical dispersion relation $\omega_{ac}(k)$, requires the asymptotic slope of $\omega_2(k)$ to be smaller than the acoustic velocity v:

$$\sqrt{\frac{\gamma D}{\beta}} < v. \tag{26}$$

This expression shows that for a given β the magnetoelastic crossing is facilitated by small exchange stiffness D and small acoustic velocity. This approximate analysis breaks down for acoustic frequencies in above-THz spectral range, where the acoustic dispersion starts deviating from its linear approximation.

Figure 5 highlights the remarkable role of exchange stiffness to achieve the dispersion crossing between nutation magnons and longitudinal acoustic phonons. Doping Py thin films with gadolinium has been shown to gradually reduce the exchange stiffness upon Gd-concentration from 300 to 100 [meV $\times$ Å^2] [13]. For a fixed value of inertial parameter $\beta = 0.276$ ps, nutation magnons for pure Py samples do not display any crossing with acoustic phonons within the displayed range of k-vectors but the Gd-doped Py with 13% Gd concentration does. The nutation magnon-phonon crossing point occurs at 0.75 THz frequency and $k = 0.85$ nm^{-1} (with a magnon wavelength of approximately 5 nm), i.e., magnon parameters readily accessible in ultrafast magnetooptical experiments [10].

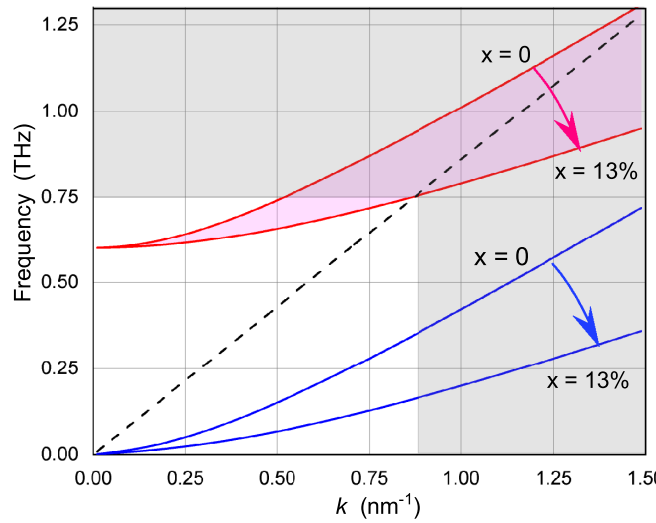

FIG. 5. The magnetoacoustic phase-matching condition for nutation magnons can be tuned via the reduction of exchange stiffness in Gd-doped Py samples. Gd concentration x varies from 0 to 13%. The dashed line displays the acoustic dispersion relation $\omega_{ac}/(2\pi)$. Magnetoelastic coupling with the precession mangon is efficient when the dashed line lies within the pink tinted area. Material parameters are taken from Ref. [13] and $\beta = 0.276$ ps.

VI. CONCLUSION

In this paper we theoretically studied exchange inertial magnons in ferromagnetic samples of different shapes under the action of an external magnetic field. The parametrization of magnetization dynamics in terms of two independent parameters, the Gilbert damping α and the inertial time β, allows for unambiguous discrimination between the inertial and damping effects as well as their impact on both branches of magnon dispersion. Inertial effects are found to strongly effect not only the frequencies (magnon eigenvalues) of both branches but also to result in a monotonous increase of the Q-factor as a function of the external magnetic field and magnon k-vector. The two magnon branches are found to process in opposite directions along the elliptical trajectories with the perpendicularly oriented long axis of the ellipses (magnon eigenvectors). Their ellipticity is found to depend on the components of the demagnetizing tensor. An analytical criterion for the existence of phase-matched magnetoelastic excitation of nutation magnons has been derived and illustrated for Gd-doped permalloy samples with tunable exchange stiffness.

ACKNOWLEDGMENTS

Financial support by the Russian Foundation for Basic Research (Grant No. 19-02-00682) and by the Agence Nationale de la Recherche (grant ANR-21-MRS1-0015 - IRON-MAG).

[1] L. D. Landau and L. M. Lifshitz, Phys. Z. Sowjetunion **8**, 153 (1935).
[2] T. L. Gilbert, Ph.D. Thesis, Illinois Institute of Technology, 1956.
[3] T. L. Gilbert, IEEE Trans. Magn. **40**, 3443 (2004).
[4] R. W. Damon and J. R. Eshbach, J. Phys. Chem. Solids **19**, 308 (1961).
[5] M. Farle, Rep. Prog. Phys. **61**, 755 (1998).

[6] L. Thevenard, J.-Y. Duquesne, E. Peronne, H. J. von Bardeleben, H. Jaffres, S. Ruttala, J.-M. George, A. Lemaitre, and C. Gourdon, Phys. Rev. B **87**, 144402 (2013).

[7] V. S. Vlasov, A. M. Lomonosov, A. V. Golov, L. N. Kotov, V. Besse, A. Alekhin, D. A. Kuzmin, I. V. Bychkov, and V. V. Temnov, Phys. Rev. B **101**, 024425 (2020).

[8] M. van Kampen, C. Jozsa, J. T. Kohlhepp, P. LeClair, L. Lagae, W. J. M. deJonge, and B. Koopmans, Phys. Rev. Lett. **88**, 227201 (2002).

[9] V. Kruglyak, S. Demokritov, and D. Grundler, J. Phys. D **43**, 264001 (2010).

[10] I. Razdolski, A. Alekhin, N. Ilin, J. P. Meyburg, V. Roddatis, D. Diesing, U. Bovensiepen, and A. Melnikov, Nat. Commun. **8**, 15007 (2017).

[11] E. Beaurepaire, J.-C. Merle, A. Daunois, and J.-Y. Bigot, Phys. Rev. Lett. **76**, 4250 (1996).

[12] A. Kirilyuk, A. V. Kimel, and T. Rasing, Rev. Mod. Phys. **82**, 2731 (2010).

[13] R. Salikhov, A. Alekhin, T. Parpiiev, T. Pezeril, D. Makarov, R. Abrudan, R. Meckenstock, F. Radu, M. Farle, H. Zabel *et al.*, Phys. Rev. B **99**, 104412 (2019).

[14] W. F. Brown, Jr., Phys. Rev. **130**, 1677 (1963).

[15] J.-E. Wegrowe and M.-C. Ciornei, Am. J. Phys. **80**, 607 (2012).

[16] In a majority of the published reports on the magnetic inertia, the coefficient used is the relaxation time τ of the inertial degrees of freedom $\tau = \beta/\alpha$, which has a clear physical meaning. However, only the parameter β is intrinsic, i.e., proper to the material. Indeed, in the framework of the mechanical analogy, β is defined by the first and second inertial moments $I_1 = I_2$, see Ref. [15].

[17] J.-E. Wegrowe, Phys. Rev. B **62**, 1067 (2000).

[18] M. Fähnle, D. Steiauf, and C. Illg, Phys. Rev. B **84**, 172403 (2011).

[19] M. Fähnle, D. Steiauf, and C. Illg, Phys. Rev. B **88**, 219905(E) (2013).

[20] M.-C. Ciornei, J. M. Rubí, and J.-E. Wegrowe, Phys. Rev. B **83**, 020410(R) (2011).

[21] S. Bhattacharjee, L. Nordström, and J. Fransson, Phys. Rev. Lett. **108**, 057204 (2012).

[22] T. Kikuchi and G. Tatara, Phys. Rev. B **92**, 184410 (2015).

[23] J.-E. Wegrowe and E. Olive, J. Phys.: Condens. Matter **28**, 106001 (2016).

[24] M. Sayad, R. Rausch, and M. Potthoff, Europhys. Lett. **116**, 17001 (2016).

[25] D. Thonig, O. Eriksson, and M. Pereiro, Sci. Rep. **7**, 1 (2017).

[26] R. Mondal, M. Berritta, A. K. Nandy, and P. M. Oppeneer, Phys. Rev. B **96**, 024425 (2017).

[27] U. Bajpai and B. K. Nikolić, Phys. Rev. B **99**, 134409 (2019).

[28] M. Fähnle, J. Magn. Magn. Mater. **469**, 28 (2019).

[29] R. Mondal and P. M. Oppeneer, J. Phys.: Condens. Matter **32**, 455802 (2020).

[30] S. Giordano and P.-M. Déjardin, Phys. Rev. B **102**, 214406 (2020).

[31] R. Mondal, S. Großenbach, L. Rózsa, and U. Nowak, Phys. Rev. B **103**, 104404 (2021).

[32] S. V. Titov, W. T. Coffey, Y. P. Kalmykov, M. Zarifakis, and A. S. Titov, Phys. Rev. B **103**, 144433 (2021).

[33] E. Olive, Y. Lansac, and J.-E. Wegrowe, Appl. Phys. Lett. **100**, 192407 (2012).

[34] E. Olive, Y. Lansac, M. Meyer, M. Hayoun, and J.-E. Wegrowe, J. Appl. Phys. **117**, 213904 (2015).

[35] D. Bottcher and J. Henk, Phys. Rev. B **86**, 020404(R) (2012).

[36] M. Cherkasskii, M. Farle, and A. Semisalova, Phys. Rev. B **102**, 184432 (2020).

[37] K. Neeraj, N. Awari, S. Kovalev, D. Polley, N. Z. Hagström, S. S. P. K. Arekapudi, A. Semisalova, K. Lenz, B. Green, J.-C. Deinert *et al.*, Nat. Phys. **17**, 245 (2021).

[38] Y. Li, A.-L. Barra, S. Auffret, U. Ebels, and W. E. Bailey, Phys. Rev. B **92**, 140413(R) (2015).

[39] I. Makhfudz, E. Olive, and S. Nicolis, Appl. Phys. Lett. **117**, 132403 (2020).

[40] V. V. Temnov, C. Klieber, K. A. Nelson, T. Thomay, V. Knittel, A. Leitenstorfer, D. Makarov, M. Albrecht, and R. Bratschitsch, Nat. Commun. **4**, 1468 (2013).

[41] V. V. Temnov, I. Razdolski, T. Pezeril, D. Makarov, D. Seletskiy, A. Melnikov, and K. A. Nelson, J. Opt. **18**, 093002 (2016).

[42] V. Besse, A. V. Golov, V. S. Vlasov, A. Alekhin, D. Kuzmin, I. V. Bychkov, L. N. Kotov, and V. V. Temnov, J. Magn. Magn. Mater. **502**, 166320 (2020).

[43] J. Janušonis, C. L. Chang, T. Jansma, A. Gatilova, V. S. Vlasov, A. M. Lomonosov, V. V. Temnov, and R. I. Tobey, Phys. Rev. B **94**, 024415 (2016).

[44] C. L. Chang, A. M. Lomonosov, J. Janusonis, V. S. Vlasov, V. V. Temnov, and R. I. Tobey, Phys. Rev. B **95**, 060409(R) (2017).